the numerical simulations, we used backward, forward and central FD schemes given by Eqs. (11)–(13) and the NSFD scheme described in Eq. (20) with $\alpha_a = \alpha_b = 0$, $\beta_a = \beta_b = 1$ and $\gamma_a = \gamma_b = -1$. The set of algebraic equations was solved using Newton–Raphson subroutine from Matlab package.

For different values of Pe and ϕ, Fig. 2 shows the E_m as a function of number of nodes N. To appreciate the effect of convective transport over the performance of the proposed numerical scheme, we consider $\phi = 2$ and four values of Pe (0.1, 1.0, 10 and 100). When the diffusive transport dominates over convective effects ($Pe < 1$), Fig. 2 shows that same maximum errors of NSFD and CFD can be observed. For the case when convective transport is more important than diffusive transport ($Pe < 1$), the NSFD presents lower E_m than all FD schemes. Particularly, for $Pe = 100$ CFD scheme shows 3 order of magnitude higher than NSFD. This result indicates that the proposed numerical scheme can reduce the numerical approximation errors that arise in processes where the global process is dominated by convective transport. On the other hand, for a constant value of Pe, the effects of the chemical reaction on the performance of numerical scheme, can be observed. Fig. 3 shows that NSFD scheme provides smaller approximation errors than the classical FD schemes. This outperforming is more important for small values of ϕ, since NSFD scheme is based on the analytic inversion of the differential operator that is related with diffusive and convective processes.

Figs. 2 and 3 indicate that, in general, NSFD and CFD schemes show approximation order of $O(h^2)$, while FFD and BFD exhibit only $O(h)$. This is because the global approximation orders of classical FD schemes depend on the convective operator approximation, i.e., if the convective operator is approximated with first-order FD, the global order is reduced to first-order. On the other hand, in the derivation of the NSFD scheme it is not necessary the approximation of the convective operator. Indeed, Green's function formulation leads, in a natural form, to a global second-order approximation.

4.1.2. Dynamical case

For this case, to obtain a reference solution of the catalytic particle model the Laplace transform was applied to Eq. (23). In this case, the analytical solution was found using the Laplace transform method and it is given by Eq. (24) with $m_1 = \sqrt{Pe^2 + 4(s + \phi^2)}/2$ and $m_2 = \sqrt{Pe^2 - 4(s + \phi^2)}/2$. Unfortunately, the inverse Laplace transform for this expression is not available. In order to determinate the solution in the time-domain, we used the numerical inversion by Zakian's algorithm (Zakian, 1975; Taiwo et al., 1995). To quantify the approximation errors, we consider the temporal maximum error (E_t) defined as

$$E_t = \sum_k^N \max \left| \frac{u_e(x_i, t_k) - u(x_i, t_k)}{u_e(x_i, t_k)} \right| \tag{26}$$

where N is the total number of time step (final time/δt), $u(x_i, t_k)$ is an approximation of the concentration profile at time $k\delta t$ and $u_e(x_i, t_k)$ is the computed value of concentration profile via numerical inversion Laplace transform using tolerances of 10^{-10}.

For $N = 50$ and different values of Pe and ϕ, Fig. 4 shows the concentration profiles and their respective E_t. As expected, for a wide range of Pe and ϕ better agreements between the reference solution and NSFD approximations are observed. This is in line
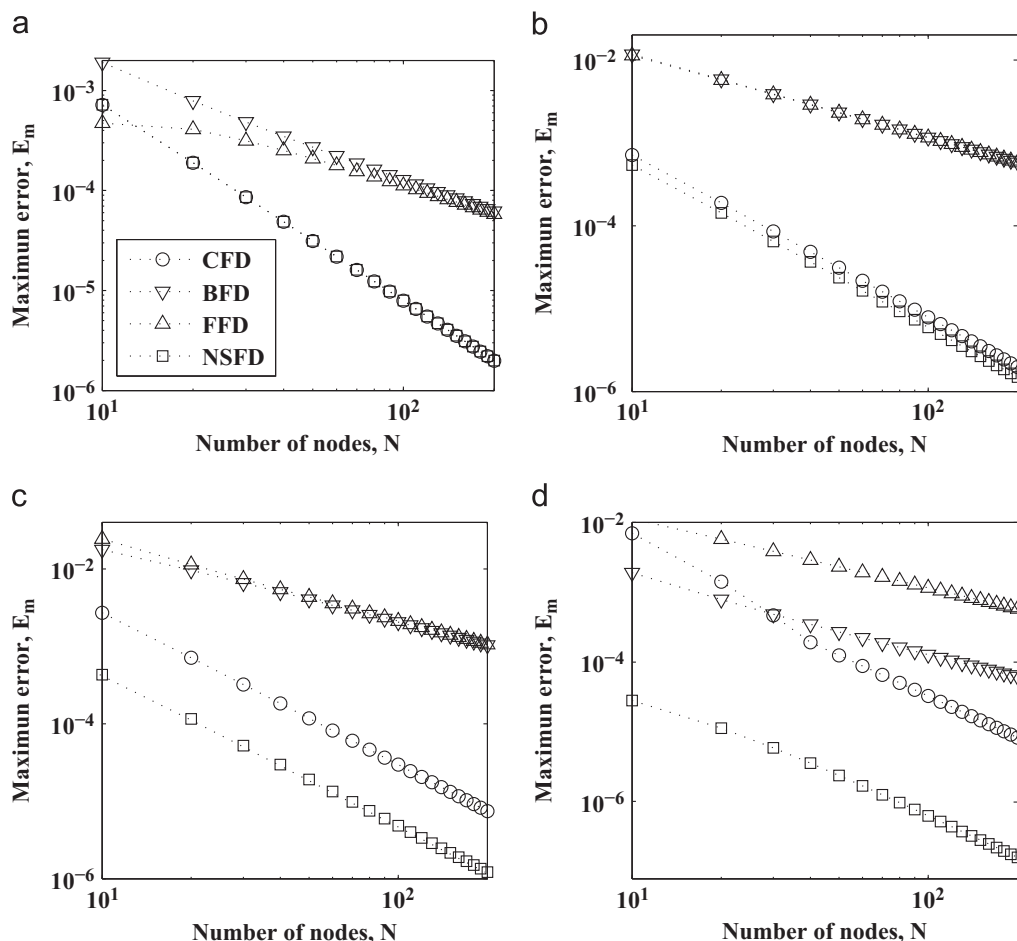

Fig. 2. Maximum error (E_m) as a function of the number of nodes (N), for $\phi = 2.0$ and (a) $Pe = 0.1$, (b) $Pe = 1.0$, (c) $Pe = 10$ and (d) $Pe = 100$.